# Curie isotherm depth from aeromagnetic data constraining shallow heat source depths in the central Aeolian Ridge (Southern Tyrrhenian Sea, Italy)

**Article** *in* Bulletin of Volcanology · March 2013

DOI: 10.1007/s00445-013-0710-9

CITATIONS
26

READS
238

**4 authors:**

Riccardo De Ritis
National Institute of Geophysics and Volcanology
**50** PUBLICATIONS **542** CITATIONS
SEE PROFILE

Dhananjay Ravat
University of Kentucky
**131** PUBLICATIONS **2,523** CITATIONS
SEE PROFILE

Ventura Guido
National Institute of Geophysics and Volcanology
**209** PUBLICATIONS **4,916** CITATIONS
SEE PROFILE

Massimo Chiappini
National Institute of Geophysics and Volcanology
**142** PUBLICATIONS **1,676** CITATIONS
SEE PROFILE

Bull Volcanol (2013) 75:710
DOI 10.1007/s00445-013-0710-9

RESEARCH ARTICLE

# Curie isotherm depth from aeromagnetic data constraining shallow heat source depths in the central Aeolian Ridge (Southern Tyrrhenian Sea, Italy)

**R. De Ritis · D. Ravat · G. Ventura · M. Chiappini**

Received: 12 April 2012 / Accepted: 5 March 2013


**Abstract** The Salina, Lipari, and Vulcano volcanic ridge and the surrounding sea sectors (Aeolian Archipelago, Southern Tyrrhenian Sea, Italy) are characterized by vents responsible for a recent (<40 ka—1889/1890 AD) effusive and explosive subareal activity and repeated, 56 to 7 ka in age, submarine explosive eruptions from source areas located between Lipari and Vulcano. A spectral depth estimation of the magnetic bottom using a fractal method on aeromagnetic data from Vulcano, Lipari, and Salina volcanic ridge allows us to constrain the Curie isotherm depth. The elevated portion of the isotherm is between 2 and 3 km below Salina and Vulcano and about 1 km below Lipari. The Curie depth results in the context of other geological and geophysical evidence suggest that the rise of the Curie isotherm is mainly due to the occurrence of shallow heat sources such as magma ponds and associated hydrothermal systems. The short-wavelength magnetic anomaly field reflects magnetic contrasts from highly magnetized volcanic bodies, low-magnetization sediments, and hydrothermally altered rocks. Borehole temperature data verify the Curie temperature derived from the magnetic methods on the island of Vulcano. We conclude that the whole Vulcano, Lipari, and Salina volcanic ridge is active and should be monitored.

**Keywords** Magnetic spectral depths · Curie isotherm · Volcanism · Tectonics · Aeolian Archipelago

Editorial responsibility: T. Ohminato

R. De Ritis · G. Ventura (✉) · M. Chiappini
Istituto Nazionale di Geofisica e Vulcanologia,
00143 Rome, Italy
e-mail: guido.ventura@ingv.it

D. Ravat
Department of Earth and Environmental Sciences,
University of Kentucky, 101 Slone Research Building,
Lexington, KY 40506-0053, USA

## Introduction

The crust below active volcanoes is generally characterized by an upwarp of isotherms due to temperature rise of mantle origin as well as shallow- to intermediate-depth volcanic sources, e.g., hydrothermal systems and/or magmatic reservoirs, leading to complex multi-modal geotherms. The thermal structure of these areas may be investigated with geological (e.g., wells) and geochemical (gas, water) methods. These methods are applicable to a local scale, i.e., to single volcanoes or calderas. At larger scales, in areas with a number of volcanic edifices, a complex crustal thermal pattern may result from the superimposed effects of multiple magmatic reservoirs at different depths. Magnetic surveying has been successfully applied to study the inner structure of volcanic areas (e.g., Finn et al. 2001; Blanco Montenegro et al. 2007) and to assess the magnetic bottom and define the Curie isotherm depth within the crust at regional scale (Chiappini et al. 2002; Aydın et al. 2005; Bouligand et al. 2009). In the Aeolian volcanic arc (Southern Tyrrhenian Sea, Italy), the occurrence of active volcanism and highly magnetic rocks together with the presence of large areas with very low values of the magnetic anomaly field (De Ritis et al. 2005, 2007) makes it conducive to examine the magnetic bottom related to possible Curie depth variations in the central sector of Aeolian Islands (Vulcano, Lipari, and Salina (VLS) islands, Italy), where partially overlapping monogenic and polygenic active volcanoes coexist. In this paper, the magnetic bottom of the VLS ridge is defined using spectral methods (Maus et al. 1997; Bouligand et al. 2009) applied to aeromagnetic datasets acquired by Istituto Nazionale di Geofisica e Vulcanologia (INGV) between 2003 and 2005. Previously, spectral magnetic bottom/Curie depth determinations have been used to understand crustal-scale temperature structures with appropriately large window sizes of generally hundreds

Published online: 20 March 2013

of kilometers or more (see references in Ravat et al. (2007); Bouligand et al. 2009; Ravat et al. 2011). They have not been used prior to this study for small isolated volcanic constructs with appropriately small window sizes to constrain the shallow thermal structure. Here, we focus on the shallow thermal structure, perform appropriate model studies, and discuss the results of our analyses of the VLS region in light of available geophysical and geological information. The approach used may be suitable for other active volcanic and/or hydrothermal areas whose anomalies can be appropriately isolated for resolving shallow structures.

## Geodynamic and volcanological setting

The Aeolian Islands and the associated volcanic seamounts are located between the Southern Tyrrhenian Sea back-arc and the Calabrian Arc orogenic belt. The volcanic rocks belong to the calcalkaline, shoshonitic, and alkaline potassic association and are younger than about 1.3 Ma (De Astis et al. 2003). The Aeolian volcanism is related to the Ionian subduction below the Calabrian Arc (Gvirtzman and Nur 2001). The western boundary of the slab is controlled by a NNW–SSE striking strike–slip fault system along which VLS formed in the last 0.4 Ma (De Rosa et al. (2003a) and reference therein; Fig. 1). This fault system cuts a Pliocene E–W elongated sedimentary basin. VLS is characterized by a crustal-scale seismicity related to the NNW–SSE faults bounding a pull-apart basin centered on Lipari and extending northward at Salina and southward at Vulcano (Mazzuoli et al. 1995). Volcanism is still active on Vulcano (Fossa Cone eruption in 1888–1890), but at Lipari the last eruption was 1230 AD and at Salina activity ceased at about 13 ka (De Rosa et al. 2003a). Hydrothermal activity and active degassing are concentrated on the Fossa Cone (Vulcano) and western Lipari, where large hydrothermally altered areas are located on faults belonging to the NNW–SSE striking fault system (Fig. 1) (Tranne et al. 2002; Boyce 2007). Submarine fumaroles occur to the west of Salina, west and east of Lipari, and northwest of Vulcano (Romagnoli et al. 1989). Sparse heat flux measurements in the Aeolian Islands range between 70 and 150 $mW m^{-2}$ (Pasquale et al. 2003). On the active VLS volcanoes, the fumarole temperature ranges between 80–90 and 340–360 °C, reaching up to 700 °C during episodes of unrest (e.g., at Fossa Cone in 1980; Granieri et al. 2006). The available seismic data (Ventura et al. 1999) show a local upwelling of the Moho below Lipari (Moho at 18–19 km b.s.l.), while at Salina and Vulcano, the Moho is at about 20–21 km b.s.l. The interface between the sedimentary and volcanic cover and the underlying Calabrian Arc rocks is located between 1 and 2.5 km b.s.l..

The subaeral volcanic activity associated with VLS is characterized by early basaltic to andesitic products from low-magnitude explosive and effusive eruptions. In the last 42 ka, dacitic to rhyolitic volcanism also occurred with effusive, extrusive, and sub-plinian explosive eruptions. Results from petrological studies (De Rosa et al. 2003b; Frezzotti et al. 2003; Zanon et al. 2003; Zanon and Nikogosian 2004; Donato et al. 2006; Peccerillo et al. 2006; Di Martino et al. 2010) allow us to characterize the VLS plumbing system (Fig. 2). At Vulcano, the magma storage zones in the last 120 ka were concentrated in the uppermost 5 km of the continental crust and between 10 and 20 km, whereas at Lipari and Salina the storage zones developed between 223 and 13 ka involved the whole crustal thickness.

Widespread ash-flow deposits of age between 56±4 ka and about 7 ka from submarine explosive eruptions outcrop on VLS (Lucchi et al. 2008). The majority of these eruptions occurred between 24 and 7 ka, and their source (vent) area has been identified on the basis of geochronological, stratigraphic, and magnetic investigations in the sea sector located west of La Fossa Cone on Vulcano (Cicchino et al. 2011).

## Data acquisition and processing

INGV carried out two helicopter-borne magnetic surveys over Vulcano, Lipari, and Salina islands and the surrounding offshore. The surveys were flown at constant barometric height encompassing the whole VLS ridge. A campaign along NE–SW profiles orthogonal to the direction of the volcanic ridge was carried out in October 2003 (inset in Fig. 3a) with a line spacing of about 1.5 km. In 2005, a new campaign was carried out with the same orientation in between the 2003 lines, reducing the spacing to 750 m. Total intensity magnetic data were acquired with an optically pumped cesium magnetometer. The surveys were conducted at a constant barometric altitude of 500 m except over areas of higher topographic relief where draped profiles were flown with constant terrain clearance of 200 m. A GPS receiver operating in differential mode was used for accurate survey navigation, and a laser altimeter at 0.3 Hz recorded the terrain clearance. A base station proton precession magnetometer located on Vulcano Island was used to remove the external magnetic field variations from observations.

The 2003 and 2005 data sets were reduced to the same geomagnetic epoch of 2003.0 using the L'Aquila Geomagnetic Observatory (central Italy) datum as reference value. The total intensity magnetic anomaly field was obtained by removing the International Geomagnetic Reference Field (IGRF) which has spherical harmonic terms including degrees and orders up to 13 (Macmillan and Maus 2005).

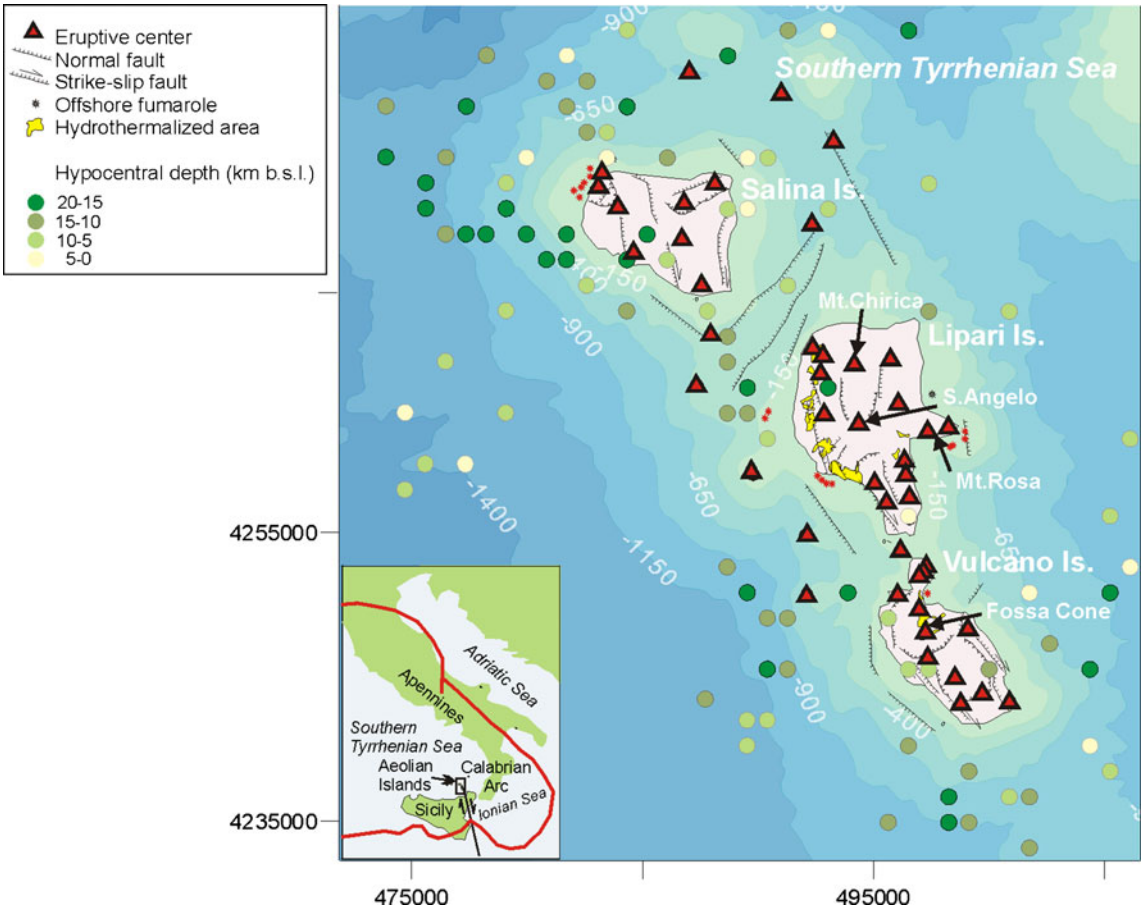


**Fig. 1** Location and structural sketch map of the central sector of the Aeolian Islands (data from Romagnoli et al. 1989; Mazzuoli et al. 1995; Ventura et al. 1999; Tranne et al. 2002). The crustal (<20 km in depth) earthquakes are from Castello et al. (2005)

Thus, the core field is precise down to approximately 2,500 km and does not leave behind any significant core field residuals in the anomaly field as is the case with the data processed with early IGRFs. Consequently, the longest wavelength in our anomaly field is primarily based on the size of the compiled database that we used (i.e., the wavelength of about 40 km), and it does not require ad-hoc long-wavelength filtering as may have been necessary when determining spectral depths from data sets acquired and processed with IGRFs prior to 2000. The data sets were merged and gridded at 1-km elevation a.s.l. with a cell size of 250 m using the minimum curvature algorithm to produce the total intensity magnetic anomaly map (Fig. 3a). The anomaly field was reduced-to-pole (RTP; Baranov and Naudy 1964) (Fig. 3b) to center the induced anomaly components over their geologic sources and thus simplify their spatial associations with crustal geology and make them less spread out from the oblique inducing inclination in the region. The RTP data allow analyses of smaller data windows on the volcanoes. The direction of remanent magnetization is very close to the direction of the present-day core field in the region since most of the short-wavelength magnetic sources were emplaced in the youngest portion of the Brunhes magnetic epoch (~780 ka to present normal geomagnetic epoch). Accordingly, the RTP transformation is also useful for simplifying spatial relationships between the region's geologic and remanent anomaly components (Blanco Montenegro et al. 2007 and De Ritis et al. 2007).

## Magnetic Curie depth

### The fractal method

We use the RTP map to derive Curie depths from the fractal method of Maus et al. (1997) and Bouligand et al. (2009) because the RTP transformation spatially focuses anomalies on their respective sources, and therefore one can consider small data windows to derive Fourier spectra to improve the resolution appropriate for volcanoes.

The basic magnetic model of the fractal method (Maus et al. 1997; Bouligand et al. 2009) has three parameters that generate model spectra: the depth to the top of the source ($Z_t$), the thickness of the magnetic layer ($T$), and the fractal

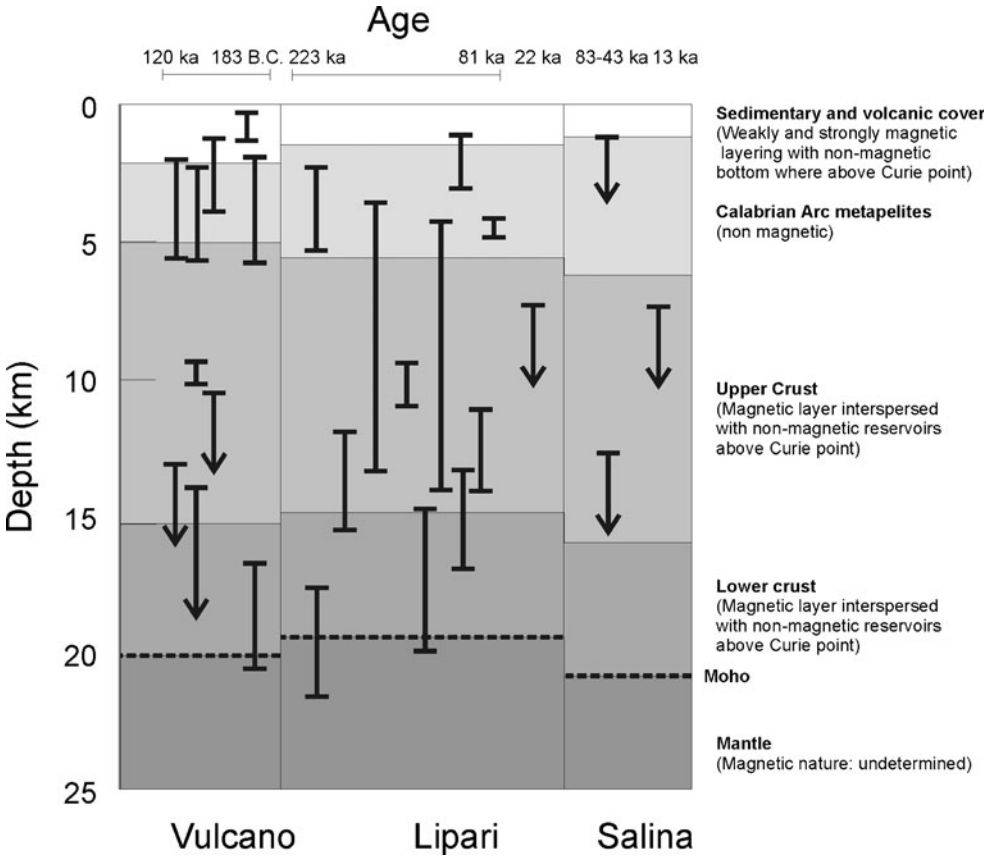


**Fig. 2** Schematic sketch showing the depth range of magmatic reservoirs and crustal layering vs age of the erupted products in VLS as deduced by petrological and geophysical studies (data from Ventura et al. 1999; De Rosa et al. 2003b; Frezzotti et al. 2003; Zanon et al. 2003; Zanon and Nikogosian 2004; Donato et al. 2006; Peccerillo et al. 2006; Di Martino et al. 2010). The nature of the magnetization distribution we envision in different crustal layers under Salina, Lipari, and Vulcano is described at the right side of the figure

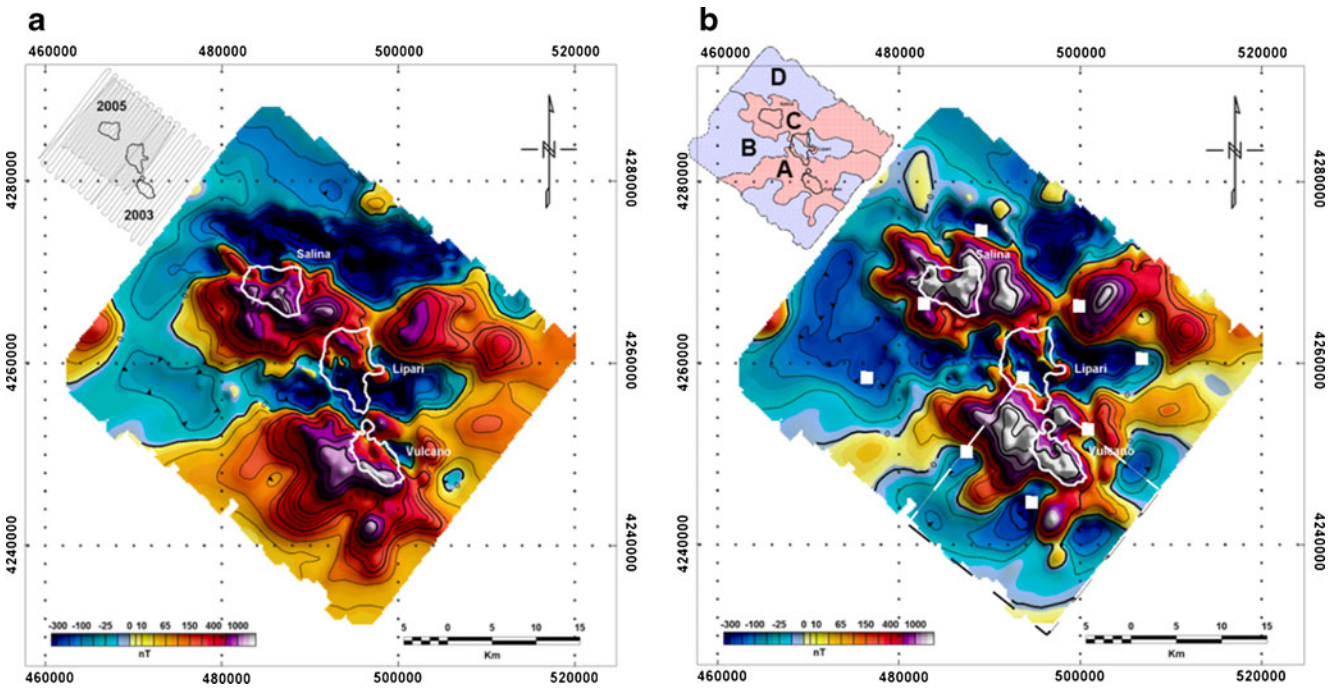


**Fig. 3** **a** Shaded relief aeromagnetic anomaly map of the VLS ridge and surrounding offshore. *Inset*, 2003 and 2005 survey flight paths. **b** Shaded Relief Reduced-to-pole aeromagnetic anomaly map assuming geomagnetic inclination of 54° and declination of 2°. The labeled RTP anomalies are discussed in the text. *Inset*, magnetic anomaly patterns *A*, *B*, *C*, and *D* of the VLS ridge region (discussed in the text). In order to compute spectral depths, the map was rotated to lie along *x*–*y* coordinates. The *dashed rectangle* represents a 20-km window situated in the lower left corner of the data in the rotated reference frame, and *white diamonds* show centers of nine windows. Windows corresponding to the last row and the last column of the map are larger; however, the computation of power spectra is based on 20-km square windows situated on the *white diamonds*

parameter (β) describing the scaling relationship of magnetization in the layer (i.e., how magnetization is correlated to its neighboring values; For example, β=0 being random magnetization, and successively higher β representing increasingly correlated magnetization to its neighbors, reaching finally the situation similar to blocks of magnetization with uniform properties used in typical magnetic modeling software). An example of the fractal model and the details of the method, including mathematics, can be found in Bouligand et al. (2009), and only the parts essential for understanding the method and its results are discussed here.

Bouligand et al. (2009) found an analytical solution for the integral derived by Maus et al. (1997) for the above one-layer model. The analytical solution allowed faster computations that made possible the application of the method to a large grid of magnetic data in a moving window manner. In their analysis of the western US magnetic anomaly data, Bouligand et al. (2009) chose to fix the fractal parameter to its most commonly encountered continental value of 3 and derived the remaining two parameters, $Z_t$ and $T$, by solving a non-linear equation leading to the minimum misfit between the azimuthally averaged observed magnetic spectra and the modeled spectra by the fractal method.

## Parameter ambiguity

Bouligand et al. (2009) calculated only parameters that led to the minimum misfit. However, for a given observed spectra, there can be a few different sets of parameters that can lead to a fit of the observed and modeled spectra nearly as good as the one having the minimum misfit (e.g., see observed and computed spectra in Fig. 4a, b which are for all practical purposes indistinguishable from one another). Such models constitute alternative feasible solutions of the fractal method and illustrate the non-uniqueness of the method that must also be taken into account when interpreting its results. Such non-uniqueness is a feature of all spectral potential field methods and originates in its basic ambiguity. The ambiguity is also implicitly present in Spector and Grant (1970) method and all its subsequent variations (Okubo et al. 1985; Fedi et al. 1997; Tanaka et al. 1999; Ravat et al. 2007; and Bansal et al. 2011) that use slope segments or peaks of spectra to derive depths of layers. It is simply harder to analyze the ambiguity in the methods involving slope segments or peaks of spectra because the forward model in these methods is a statistical ensemble model rather than an analytical model that generates spectra from specific parameters (e.g., the forward model generated by the fractal method). The ambiguity can only be reduced by having constraining corollary information in the region. In lieu of such constraints, the entire parameter space must be examined for acceptable solutions; thus, a range of acceptable solutions is all one can determine.

## Model study for restricting parameter range

In this study, we used inferences from model studies previously performed and explained in Ravat et al. (2011) and also performed new model studies for thin near-surface magnetic layers appropriate for simulating magnetic layers above the Curie temperature of magnetic minerals (see Table 1). The model studies are performed to see how the method works in ideal situations. In the new model study (Table 1), we tested several situations: window sizes of 20 and 50 km and several layer thicknesses ($T$) ranging from 1 to 10 km. We report the cases solved for the minimum misfit between the observed spectra and the spectra computed from all three parameters, $Z_t$, $T$, and β (under rows called "Inverted unconstrained—3 para"). As seen from Fig. 6 of Bouligand et al. (2009), the derived parameters $Z_t$ and β are strongly correlated, which means that the error in derivation of one of them will lead to compensating an error in the other. We found that in the unconstrained three-parameter cases, the depth to the top ($Z_t$) and layer thickness ($T$) leading to minimum misfit between the observed and computed spectra are nearly always underestimated than the true values of $Z_t$ and $T$, except in one case in Table 1. The fractal parameter, β, is always over-estimated as a result of the compensation of the error in $Z_t$. The main point we are making here is that the minimum misfit between the observed and computed spectra (a quantitative measure) does not necessarily lead to the correct solution in this method; solutions from other near-equally fitting calculated spectra must also be considered in the interpretation, and constraints from other geologic and geophysical information must be used in narrowing down the plausible range of parameters.

There are also other complexities that deter us from solely relying on a quantitative measure such as the minimum L1 or L2 measure of misfit. For example, in some cases, the computed spectra from such minimum misfit solutions may not fit well the observed spectra at all, and in such cases, no solution might be acceptable. In other cases, one or more wavenumber segments in the computed spectra might have, visually, unacceptably different slopes or fit than the observed spectra and so may be unusable for the purpose of determining model parameters. Even though the judgment about the reasonability of the visual fit is subjective, it is an important consideration when using this method because the combination of $Z_t$, $T$, and β determines the characteristics of the computed spectra and the validity of the solution depends on the goodness of overall fit to the observed spectra and not simply the minimum of L1 or L2 measure of the misfit function. Moreover, there are several norms one can use for assessing misfit. Although we show

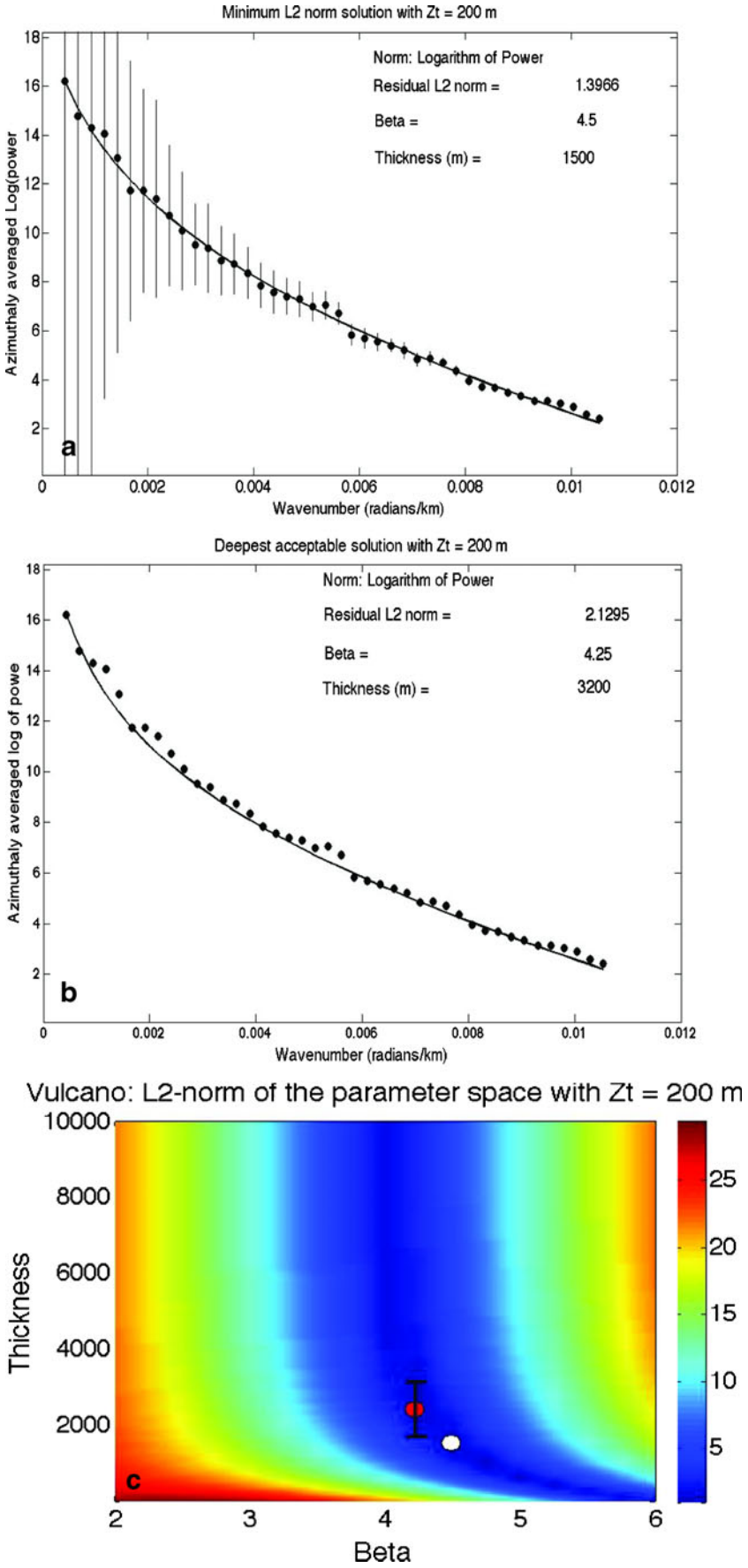


**Fig. 4** **a** Spectra from the minimum root mean square between the observed and the modeled spectra from a 20-km window over Vulcano when $Z_t$ is constrained based on forward modeling of the high-wavenumber part of the spectra (see the text for details). *Solid dots* are the observed spectrum, and the *solid curve* is the modeled spectrum. The solution parameters are indicated in the figure. **b** The deepest acceptable solution from the same window over Vulcano. **c** Residual L2-norm tradeoffs space for the solutions constrained with $Z_t$=200 m. *White circle*, minimum L2-norm solution when $Z_t$=200 m (spectra shown in Fig. 4a); *red circle*, other nearly equally well-fitting computed spectra with the range of thicknesses indicated by the *error bar* (an example of the deepest acceptable solution is shown in Fig. 4b)

**Table 1** Model study for thin near-surface magnetic layers specially conducted for the situation encountered in this study. A crustal scale model study can be found in Ravat et al. (2011)

| Window size (m)/grid spacing (m) | $20\times10^3/250$ | $20\times10^3/250$ | $50\times10^3/250$ | $20\times10^3/250$ | $20\times10^3/250$ | $50\times10^3/250$ |
|---|---|---|---|---|---|---|
| True $Z_t$ (m) | 1,000 | 1,000 | 1,000 | 1,000 | 1,000 | 1,000 |
| True $T$ (m) | 1,000 | 3,000 | 3,000 | 5,000 | 10,000 | 5,000 |
| True β | 3 | 3 | 3 | 3 | 3 | 3 |
| Inverted, unconstrained—3 para: $Z_t$ (m) | 700 | 700 | 900 | 2,000 | 700 | 800 |
| Inverted, unconstrained—3 para: $T$ (m) | 900 | 1,400 | 2,000 | 5,000 | 5,000 | 2,000 |
| Inverted, unconstrained—3 para: β | 3.5 | 3.25 | 3.25 | 4.5 | 3 | 3.75 |
| Range of acceptable $Z_t$ (m)[a] | 600–800 | 600–800 | 900–1,100 | 800 (β fixed) | 500–800 | 700–1,000 |
| Range of acceptable $T$ (m)[a] | 700–1,000 | 800–3,800 | 2,000–7,000 | 3,000–6,000 (β fixed) | 1,000–open-ended[b] | 1,000–8,000 |
| Range of acceptable β[a] | 3.5–4 | 2.5–3.75 | 2.25–3.25 | 3 (β fixed) | 2.75–4.5 | 2.75–4.5 |

[a] Not all solutions across the range of $Z_t$, $T$, and β are acceptable in terms of visual fit

[b] Open-ended solution is expected for this case because the model layer thickness is larger than what can be resolved with the given window size

only L2 norm in the present paper, we have computed L1 and L2 norms for all our solutions, and we find that the minimum of the misfit of the L1 norm is always different than that of the L2 norm. At the moment, we have no compelling theoretical or practical argument to choose either the L1 or the L2 misfit norm in this problem, but we do think that the overall appearance of the fit of the computed spectra to the observed one, albeit subjective, is important in choosing the derived range of solutions in this method.

In Table 1, under the rows "Range of acceptable $Z_t$", "Range of acceptable $T$", or "Range of acceptable β", we show also the range of these parameters that produce nearly similar appearing computed spectra due to non-uniqueness described in the previous paragraph. The similarity is gauged in this study in two ways: by observing how closely the computed spectra fit to the observed spectra, subject to qualitative acceptable fit criteria described earlier, and also by ascertaining that the RMS difference values of the observed and the computed spectra are small and reasonably close to the minimum misfit value. The range of parameters that lead to spectra similar in appearance to the minimum misfit spectra can be large. This indicates the uncertainty of the method when using small windows, especially when determining the thickness of thicker layers. With small windows, bottoms of thick layers cannot be determined. Our model study in Table 1 shows that 20-km wide windows with 250-m grid spacing (similar to the spacing of our grid) are adequate to resolve magnetic layers up to 5 km in thickness. For thicker and deeper magnetic layers, one would have to employ larger windows (e.g., Ravat et al. 2011), and this is consistent with the expectation of the potential field theory and experience of other researchers with this method (Maus et al. 1997; Bouligand et al. 2009).

## Data analyses without constraints

Bouligand et al. (2009), after computing results for different size windows and different values of β, chose to preselect β (β = 3) which they argued was reasonable for the continental western USA situation. However, this assumption leads to unreasonably shallow magnetic bottoms in many regions of their study and therefore cannot be correct. We instead varied all three parameters and evaluated L1 and L2 as well as visual subjective misfits between the observed and modeled spectra for data windows situated over Salina, Lipari, and Vulcano. To consider alternative feasible models, we determine the L2 measure of misfit between the observed spectra and the modeled spectra for each combination of the three parameters ($Z_t$, $T$, and β) as well as generated plots comparing their visual subjective fit. Since spectra can have noise, visual evaluation of the fit of the observed to the model allows one to consider a realistic range of models that may be acceptable rather than considering only the minimum quantitative misfit model as the best solution.

In the three-parameter unconstrained solutions that we obtained, the β values are between 4 and 5, which are more consistent with the larger magnetization correlation length expected from larger-dimension crystalline rocks of uniform

magnetization in the oceanic and the volcanic island settings. Similar high β values are also common in other volcanic situations of similar scale (Pilkington and Todoeschuck 1993; Maus and Dimri 1996; and Maus et al. 1997). In these solutions, our derived $Z_t$~200–300 m is more influenced by amplitudes at higher wavenumbers arising from the island portions of the azimuthally averaged spectra which are closer to the flight altitude than the submerged portions of the survey. As the estimated $Z_t$ is close to the flight altitude, the derived thickness range in these solutions, $T$~800–2500 m, can be taken here as the estimate of the approximate magnetic bottom. As will be discussed later, in conjunction with the known magnetic mineralogy, the derived magnetic bottoms in this study are likely to be due to the influence of the Curie temperature phenomenon rather than inherently non-magnetic basement petrology. The parameter range obtained here without restricting the three parameters is still large. In the next subsection, we introduce a restriction on $Z_t$ in order to further constrain the parameter range.

## Curie depths/magnetic bottom beneath VLS

We analyzed spectra from 20-km windows centered individually over the region of Salina (NNW), Lipari (Central), and Vulcano (SSE) islands. Because parameters β and $Z_t$ from the fractal method are dependent/correlated (Bouligand et al. 2009), we constrained $Z_t$ by forward modeling, i.e., adjusting the visual fit only to the high wavenumber part of the spectra. This estimate of $Z_t$ is lower than the flight altitude with respect to the average topography/bathymetry in the region, but it is consistent when one takes into account the draping of surveys over the islands as discussed in the previous paragraph. High amplitudes at high wavenumbers from the draped survey and noise in the short-wavelength data modify the overall high wavenumber character of the spectra, making the slopes ($Z_t$) shallower than they should be.

The results of our detailed analysis of the high resolution magnetic data of the VLS islands, which carefully explored the parameter space for thickness and β and obtained ranges of plausible solutions, are summarized in Table 2. The observed and modeled spectra for the minimum root mean square between the observed and computed spectra at Vulcano are shown in Fig. 4a, and the solution whose bottom is the deepest among the acceptable solutions for Vulcano (SSE region) is shown in Fig. 4b. As the tradeoff curve in Fig. 4c shows, there is a range of thickness estimates (the red circle and the vertical range bar) that appear as good as the minimum norm solution (the white circle). The deeper range of magnetic bottom depths obtained at Vulcano agrees with the higher temperatures observed by Faraone et al. (1986) in a borehole within a monzogabbroic intrusion (~419 °C at ~2 km depth and a titanomagnetite mineralogy whose Curie temperature is in the range 550°± 30 °C based on Zanella and Lanza (1994)). Our spectral depth estimates (Table 2) suggest that the central region of the VLS islands (Lipari) has an elevated temperature of around 550–580 °C at ~1-km depth, and this isotherm dips toward SSE toward Vulcano to around 1.5–3.0-km depth and NNW toward Salina to around 2–3-km depth. A study conducted on 900 specimens concerning nearly all the VLS lithotypes highlights that *Jr*, the remanence, is virtually unchanged up to about 400 °C (the magnetic blocking temperature which allows retention of remanent magnetizations, thermal as well as chemical and viscous, if present, in the same direction as the induced magnetization), followed by a rapid fall with depth (Zanella and Lanza 1994).

In Fig. 5, we show automatically determined magnetic bottoms from the minimum misfit spectra obtained from 20-km-width moving windows offset by 10 km (i.e., in this approach, windows are not optimally centered over geologic features/provinces of interest, and therefore the results are less precise than when one centers the window according to known geology and also analyzes the parameter space for each window). A similar moving window strategy was used by Bouligand et al. (2009) in the western USA to determine magnetic bottom/Curie depth surface by a priori choosing β=3. Constraining β in this manner is inappropriate for our study because the magnetization scale length for shallow volcanic layers can be variable (as seen in Table 2 and Bouligand et al. (2009)), and hence we derived all three parameters, using the minimum misfit criterion, from moving windows by half the window size in both directions. We present this result (Fig. 5) to represent the approximate

**Table 2** Spectral magnetic depth acceptable results over the VLS islands based on careful evaluation of the fit between observed and modeled spectra from 20-km windows

| Area | Depth to magnetic top with respect to average flight elevation ($Z_t$) (km)—the parameter constrained based on forward modeling | Depth to magnetic bottom ($Zb=Z_t+T$)—acceptable range (km) | Fractal parameter—acceptable range (β) |
|---|---|---|---|
| Salina or NNW | 0.5 | 2.0–3.3 | 3–3.25 |
| Lipari or Central | 0.2 | 1.0 | 5 |
| Vulcano or SSE | 0.2 | 1.5–3.2 | 4.25–4.5 |

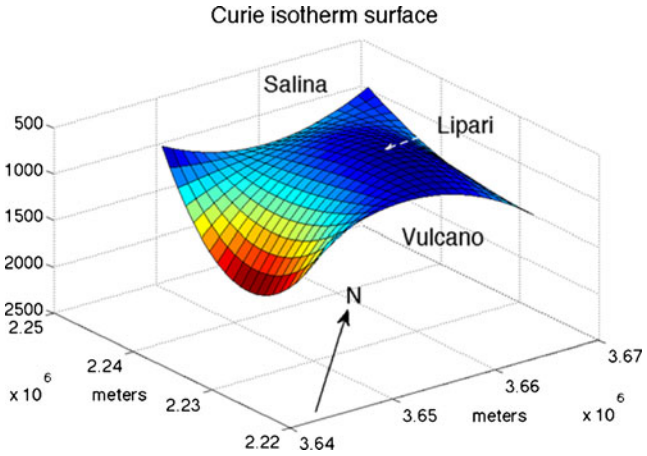


**Fig. 5** Minimum L2 norm-based magnetic bottom surface from 20-km width windows offset by 10 km, leading to a total of nine magnetic bottom determinations. Automatically moved windows are not optimally placed over anomaly features as we have done with the results in Table 2. The minimum L2 norm solutions always tend to be shallower, but they illustrate geologic variation (see also the results of Bouligand et al. (2009)). For example, for the saddle of upwarp under Vulcano, Lipari, and Salina, the automatic solutions give 1.1, 0.9, 1.1 km magnetic bottom depth, respectively, instead of 1.5–3.2, 1, and 2–3.3 km in Table 2, respectively. The deepest automatically derived magnetic bottom (*red color*) is at 2 km in depth by comparison

shape of the magnetic bottom/Curie isotherm surface. Overall, based on the results of the model study in Table 1, the model study in Ravat et al. (2011), and the example from Vulcano in Fig. 4c, we have found that the automatic solutions such as the ones in Fig. 5 have a bias toward inferring magnetic tops and bottoms shallower than they actually are in the models. Despite this limitation, automatic solutions over a grid of data can lead to useful understanding of the relative variation in the magnetic bottom/Curie depth as long as care is taken to validate the relative variation of the solutions (here we validate the relative variation using the results in Table 2). The surface in Fig. 5 shows the upwarp of magnetic bottom/Curie depth over Lipari and Vulcano in comparison to Salina and the surrounding regions. This observation is indirectly corroborated by the average shallower depth of the magma reservoirs below Lipari and Vulcano with respect to Salina (see Fig. 2).

## Discussion

The crust of the VLS ridge is probably characterized by an upwarp of isotherms due to deeper temperature rise of mantle origin as well as shallow- to intermediate-depth volcanic sources, e.g., hydrothermal systems and/or magmatic reservoirs, leading to complex multi-modal geotherms. We have focused in this paper on the shallow temperature field. The VLS anomaly field is characterized by a wide range of wavelengths and intensities (Fig. 3a). The occurrence of non-magnetic crystalline and metamorphic basement below VLS (Barberi et al. 1994) allows us to constrain the depth of the magnetic sources to the shallower Pliocene–Holocene 1–2.5-km thick sedimentary/volcanic cover. The spectral bottom estimates of the area gives magnetic layer depths between 1 and 3.3 km, consistent with the available seismic data (Ventura et al. 1999). Based on the results of Table 2 and the deeper depth of the non-magnetic Calabrian Arc basement under Lipari, we conclude that shallower magnetic bottom depth may be associated with the upwarp of the Curie isotherm surface. Under Vulcano, the magnetic bottom cannot be distinguished from the seismically determined depth to the Calabrian Arc basement. Independent results of Faraone et al. (1986) at Vulcano certainly suggest that the temperature rise above the Curie isotherm is the likely cause here. For lack of additional observed borehole temperature data at Salina, we cannot clearly differentiate the magnetic bottom from a raised Curie isotherm and the Calabrian Arc of non-magnetic basement.

In the inset of Fig. 3b, we group related anomalies into sectors labeled A, B, C, and D. The VLS magnetic pattern includes: (a) two main NW–SE to WNW-ESE elongated positive anomaly sectors located in the area of Vulcano (A) and Salina (C) and (b) two east–west-oriented negative anomaly sectors in the area of Lipari (B) and north Salina offshore (D). A synthetic magnetic model of the shallow crust under Lipari and Salina is reported in De Ritis et al. (2007), where the effect of four E–W striking bands with alternating 0 and 2.6 A/m magnetization values reasonably reproduces the real data. This four-band model and the RTP magnetic anomaly field (Fig. 3b) indicate that the positive anomaly sectors A and C may be related to highly magnetized volcanic shallow sources and intra-crustal intrusive bodies, whereas the negative anomaly sector D reflects the presence of non-magnetic materials (De Ritis et al. 2007).

Interpretation of the negative anomaly sector B is more problematic and has never been analyzed to date. Several possible factors could produce this pattern, but not all are pertinent to the study area. They include (a) sources with reverse magnetization, (b) low magnetization and/or demagnetized rocks possibly altered by hydrothermal activity, and (c) shallow magmatic reservoirs causing a local upwarping of the Curie isotherm. We reject hypothesis "a" because the Lipari terrains are younger than 223 ka, and the 92–102 ka age of the S. Angelo volcano (De Rosa et al. 2003a) in the central sector of the island lies within the present Bruhnes geomagnetic polarity epoch. We also exclude the widespread occurrence of low-magnetization rocks suggested in hypothesis "b" because of the ubiquitous presence of high 3–4-A/m magnetization S. Angelo lavas (Zanella et al. 1994). On the other hand, occurrence of

non-magnetic rocks cannot be ruled out because of the hydrothermal alteration on Lipari. In particular, the western boundary of the negative anomaly B on Lipari overlaps the fault zone where the hydrothermal activity is concentrated (Figs. 1 and 3b; Mazzuoli et al. 1995). This zone represents the pathway along which the hydrothermal fluids rise up toward the surface (Bruno et al. 2000). It is worth noting that the shorter-wavelength positive magnetic anomalies on Mt. Chirica and Mt. Rosa basaltic volcanoes in sector B (Fig. 1) align along the NW–SE direction and highlight the non-hydrothermally altered rocks of these magnetized edifices (Fig. 3b). Regarding hypothesis "c", our results show that the magnetic bottom below Lipari is at about 1-km depth, whereas at Vulcano and Salina it is located at 1.5–3.2 and 2–3.3 km, respectively. Below Lipari, the Calabrian Arc rocks are deeper than 2.5 km (Ventura et al. 1999). Since the magnetic bottom estimation is shallower than the boundary of the non-magnetic basement unit, we infer that the magnetic bottom below this island may represent the Curie isotherm depth. We propose that the broader negative anomaly sector B may involve both hydrothermally demagnetized rocks and raised isotherms below the Lipari volcanoes.

Wang et al. (1989) estimate in the VLS area the temperature of 200 °C at 10-km depth primarily associated with the mantle upwarp. Our data (magnetic bottom depths) show that the temperature at 1.5–3-km depth is in the range of 550–580 °C (titanomagnetite–magnetite Curie temperature). This result suggests a local shallow zone of ponding of hot magma that is not related to the upwarp of the mantle. Our results are compatible with the geochemical and geophysical data available for Vulcano, which indicate a reservoir at about 1,000–1,050 °C at 3.5–4 km depth and an overlying hydrothermal system at 2-km depth (Nuccio and Paonita, 2001; Ferrucci et al. 1991). We, thus, propose that the estimated depth of the magnetic bottom at Lipari represents the shallower isotherm of the Curie temperature in VLS, possibly aided by a shallow reservoir and by hydrothermal activity along faults in the magnetic trough between Vulcano and Salina where a pull-apart structure has been recognized (Mazzuoli et al. 1995). This conclusion is supported by available seismic data (Castello et al. 2005; Gambino et al. 2012), which show a smaller number of events below Lipari with respect to the Vulcano and Salina sectors, where the earthquakes are also deeper (Fig. 1). Such features may be related to the occurrence of "softer" (e.g., melts/high temperature fluids) material in the VLS central sector.

## Conclusions

The results of this study indicate the presence of shallow magmatic and hydrothermal reservoirs below VLS. These reservoirs, possibly driven by a fault system between North Vulcano and central Lipari, are located within the uppermost Calabrian Arc crystalline rocks. The Curie isotherm depth is between 2 and 3 km below Salina and Vulcano and about 1 km below Lipari. Together with the other geophysical and geologic observations, we suggest that hazard evaluation related to possible eruptions and/or hydrothermal explosions as being done over Vulcano should also be extended to Lipari and the surrounding sea sectors, where vents responsible for recent (24–7 ka) explosive eruptions have been recognized (Lucchi et al. 2008). In the cases of Vulcano and Salina, where the cause of the magnetic bottom cannot be clearly ascribed to the Curie temperature effect because of the presence of non-magnetic Calabrian basement at roughly the same depths, the spectral magnetic bottom (due to either the Curie temperature or the non-magnetic Calabrian basement) has been effectively identified using small windows for isolated anomalies of the shallow volcanic fields.

**Acknowledgments** This study was funded by INGV. Discussions with colleagues of INGV and Cosenza, Catania, Bologna, Napoli Universities were appreciated. We thank two anonymous reviewers for their thoughtful and perceptive comments and suggestions. We also thank the Associate Editor, Dr. Takao Ohminato, for his comments, suggestions, and editorial handling. All of these reviews improved the logic, the defense of arguments, and the non-expert readability of the paper substantially.

## References

Aydın I, Karat HI, Koçak A (2005) Curie-point depth map of Turkey. Geophys J Intern 162:633–640

Bansal AR, Gabriel G, Dimri VP, Krawczyk CM (2011) Estimation of depth to the bottom of magnetic sources by a modified centroid method for fractal distribution of sources: an application to aeromagnetic data in Germany. Geophysics 76:L11–L22

Baranov V, Naudy H (1964) Numerical calculation of the formula of reduction to the magnetic pole. Geophysics 29:67–79

Barberi F, Gandino A, Gioncada A, La Torre P, Sbrana A, Zenucchini C (1994) The deep structure of the Eolian arc (Filicudi–Panarea–Vulcano sector) in light of gravity, magnetic and volcanological data. J Volcanol Geotherm Res 61:189–206

Blanco Montenegro I, De Ritis R, Chiappini M (2007) Imaging and modelling the subsurface structure of volcanic calderas with high-resolution aeromagnetic data at Vulcano (Aeolian Islands, Italy). Bull Volcanol 69(6):643–659. doi:10.1007/s00445-006-0100-7

Bouligand C, Glen JMG, Blakely RJ (2009) Mapping Curie temperature depth in the western United States with a fractal model for crustal magnetization. J Geophys Res 114:B11104. doi:10.1029/2009JB006494

Boyce A (2007) Fluids in early stage hydrothermal alteration of high-sulfidation epithermal systems: a view from the Vulcano active hydrothermal system (Aeolian Island, Italy). J Volcanol Geotherm Res 166(2):76–90

Bruno PP, Paoletti V, Grimaldi M, Rapolla A (2000) Geophysical exploration for geothermal low enthalpy resources in Lipari Island, Italy. J Volcanol Geotherm Res 98:173–188

Chiappini M, Ferraccioli F, Bozzo E, Damaske D (2002) Regional compilation and analysis of aeromagnetic anomalies for the Transantarctic Mountains–Ross Sea sector of the Antarctic. Tectonophysics 347:121–137

Castello B, Selvaggi G, Chiarabba C, Amato A (2005) Catalogo della sismicità Italiana—CSI 10, 1981–2002, Cent Naz Terremoti, Ist Naz di Geofis e. Vulcanol, Rome

Cicchino AMP, Zanella E, De Astis G, Lanza R, Lucchi F, Tranne CA, Airoldi G, Mana S (2011) Rock magnetism and compositional investigation of Brown Tuffs deposits at Lipari and Vulcano (Aeolian Islands—Italy). J Volcanol Geotherm Res 208:23–38. doi:10.1016/jjvolgeores201108007

De Astis G, Ventura G, Vilardo G (2003) Geodynamic significance of the Aeolian volcanism (Southern Tyrrhenian Sea, Italy) in light of structural, seismological and geochemical data. Tectonics 22:1040. doi:10.1029/2003TC001506

De Ritis R, Blanco-Montenegro I, Ventura G, Chiappini M (2005) Aeromagnetic data provide new insights on the volcanism and tectonics of Vulcano Island and offshore areas (southern Tyrrhenian Sea, Italy). Geophys Res Lett 32:L15305. doi:10.1029/2005GL023465

De Ritis R, Ventura G, Chiappini M (2007) Aeromagnetic anomalies reveal hidden tectonic and volcanic structures in the central sector of the Aeolian Islands, southern Tyrrhenian Sea, Italy. J Geophys Res 112:B10. doi:10.1029/2006JB004639

De Rosa R, Guillou H, Mazzuoli R, Ventura G (2003a) New unspiked K–Ar ages of volcanic rocks of the central and western sector of the Aeolian Islands: reconstruction of the volcanic stages. J Volcanol Geotherm Res 120:161–178

De Rosa R, Donato P, Gioncada A, Masetti M, Santacroce R (2003b) The Monte Guardia eruption (Lipari, Aeolian Islands): an example of reversely zoned magma mixing sequence. Bull Volcanol 65:530–543

Di Martino C, Frezzotti M, Lucchi F, Peccerillo A, Tranne C, Diamond LW (2010) Magma storage and ascent at Lipari Island (Aeolian Archipelago, Southern Italy) at 223–81 ka: the role of crustal processes and tectonic influence. Bull Volcanol 72(9):1061–1076

Donato P, Behrens H, De Rosa R, Holtz F, Parat F (2006) Crystallization conditions in Upper Pollara (Salina Island, Southern Tyrrhenian Sea) magma chamber. Mineral Petrol 86:89–108

Faraone D, Silvano A, Verdiani G (1986) The monzogabbroic intrusion in the island of Vulcano, Aeolian Archipelago, Italy. Bull Volcanol 48:299–307

Fedi M, Quarta T, de Santis A (1997) Inherent power-law behavior of magnetic field power spectra from a Spector and Grant ensemble. Geophysics 62:1143–1150

Ferrucci F, Gaudiosi G, Milano G, Nercessian A, Vilardo G, Luongo G (1991) Seismological exploration of Vulcano (Aeolian Islands, Southern Tyrrhenian Sea): case history. Acta Vulcanol 1:143–152

Finn C, Sisson TW, Deszcz-Pan M (2001) Aerogeophysical measurements of collapse–prone hydrothermally altered zones at Mount Rainer volcano. Nature 409:600–603

Frezzotti ML, Peccerillo A, Bonelli R (2003) Magma ascent rates and depths of magma reservoirs beneath the Aeolian volcanic arc (Italy): inferences from fluid and melt inclusions in crustal xenoliths. In: Bodnar B, De Vivo B (eds) Melt inclusions in volcanic systems. Elsevier, Amsterdam, pp 185–206

Gambino S, Milluzzo V, Scaltrito A, Scarfì L (2012) Relocation and focal mechanisms of earthquakes in the south-central sector of the Aeolian Archipelago: new structural and volcanological insights. Tectonophysics 524/525:108–115. doi:10.1016/jtecto201112024

Granieri D, Carapezza ML, Chiodini G (2006) Correlated increase in $CO_2$ fumarolic content and diffuse emission from La Fossa crater (Vulcano, Italy): evidence of volcanic unrest or increasing gas release from a stationary deep magma body? Geophys Res Lett 33:L13316. doi:10.1029/2006GL026460

Gvirtzman Z, Nur A (2001) Residual topography, lithospheric thickness, and sunken slabs in the central Mediterranean. Earth Planet Sci Lett 187:117–130

Lucchi F, Tranne CA, De Astis G, Keller J, Losito R, Morche W (2008) Stratigraphy and significance of Brown Tuffs of the Aeolian Islands (southern Italy). J Volcanol Geotherm Res 117:49–70

Macmillan S, Maus D (2005) International geomagnetic reference field—the tenth generation. Earth Planets Space 57:1135–1140

Maus S, Gordon D, Fairhead D (1997) Curie-temperature depth estimation using a self-similar magnetization model. Geophys J Intern 129:163–168. doi:10.1111/j1365-246X1997tb00945x

Maus S, Dimri VP (1996) Depth estimation from the scaling power spectrum of potential fields? Geophys J Int 124:113–120

Mazzuoli R, Tortorici L, Ventura G (1995) Oblique rifting in Salina, Lipari and Vulcano islands (Aeolian Islands, southern Italy). Terra Nova 7:444–452

Nuccio PM, Paonita A (2001) Magmatic degassing of multicomponent vapors and assessment of magma depth: application to Vulcano Island (Italy). Earth Planet Sci Lett 193(3–4):467–481

Okubo Y, Graf RJ, Hansen RO, Ogawa K, Tsu H (1985) Curie-point depths of the island of Kyushu and surrounding areas, Japan. Geophysics 50:481–494

Pasquale V, Verdoya M, Chiozzi P (2003) Heat-flux budget in the southeastern continental margin of the Tyrrhenian basin. Phys Chem Earth 28:407–420

Peccerillo A, Frezzotti ML, De Astis G, Ventura G (2006) Modeling the magma plumbing system of Vulcano (Aeolian Islands, Italy) by integrated fluid-inclusion geobarometry, petrology, and geophysics. Geology 34:17–20

Pilkington M, Todoeschuck JP (1993) Fractal magnetization of continental crust. Geophys Res Lett 20:627–630

Ravat D, Salem A, Abdelaziz AMS, Elawadi E, Morgan P (2011) Probing magnetic bottom and crustal temperature variations along the Red Sea margin of Egypt. Tectonophysics 510:337–344

Ravat D, Pignatelli A, Nicolosi I, Chiappini M (2007) A study of spectral methods of estimating the depth to the bottom of magnetic sources from near-surface magnetic anomaly data. Geophys J Int 169:421–434

Romagnoli C, Calanchi N, Gabbianelli G, Lanzafame G, Rossi PL (1989) Contributi delle ricerche di geologia marina alla caratterizzazione morfostrutturale ed evolutiva dei complessi vulcanici di Salina, Lipari e Vulcano (Isole Eolie). Boll Gruppo Nazionale Vulcanologia 1989:971–978 (in italian)

Spector A, Grant FS (1970) Statistical models for interpreting aeromagnetic data. Geophysics 35:293–302

Tanaka A, Okubo Y, Matsubayashi O (1999) Curie point depth based on spectrum analysis of the magnetic anomaly data in East and Southeast Asia. Tectonophysics 306:461–470

Tranne CA, Lucchi F, Calanchi N, Lanzafame G, Rossi PL (2002) Geological map of the Island of Lipari (Aeolian Islands), scale 1:10000. University of Bologna and INGV, LAC Firenze

Ventura G, Vilardo G, Milano G, Pino NA (1999) Relationships among crustal structure, volcanism and strike–slip tectonics in the Lipari–Vulcano volcanic complex (Aeolian Islands, Southern Tyrrhenian Sea, Italy). Phys Earth Planet Inter 116(1–4):31–52

Wang C, Hwang W, Shi Y (1989) Thermal evolution of a rift basin: the Tyrrhenian Sea. J Geophys Res 94(B4):3991–4006

Zanella E, Lanza R (1994) Remanent and induced magnetization in the volcanites of Lipari and Vulcano (Aeolian Islands). Annals Geophys 37:1149–1156

Zanon V, Frezzotti ML, Peccerillo A (2003) Magmatic feeding system and crustal magma accumulation beneath Vulcano Island (Italy): evidence from $CO_2$ fluid inclusions in quartz xenoliths. J Geophys Res 108:2298–2301. doi:10.1029/2002JB002140

Zanon V, Nikogosian IK (2004) Evidence of crustal melting events below the Island of Salina (Aeolian Arc, Southern Italy). Geol Mag 141:525–540